Altitude and Motion Estimation for Autonomous Vehicles through Wide-Field-Integration of Optic Flow

By Ryusuke NAKATA,[1)] Naoto KOBAYASHI,[1)] Mai BANDO,[1)] and Shinji HOKAMOTO[1)]

[1)]*Department of Aeronautics and Astronautics, Kyushu University, Fukuoka, Japan*

(Received June 21st, 2017)

This study proposes an estimation method not only velocity dependent motion variables but also altitude information of a vehicle. For the estimation of the variables, Wide-Field-Integration (WFI) of optic flow algorithm is applied to image data obtained by onboard cameras. In this paper, first optic flow representations for vehicle motion is extended so that they are applicable to images obtained by cameras off from the mass center of a vehicle. Then, to make the altitude estimation possible, the extended procedure is applied to optic flow obtained by two cameras: one is placed at mass center of a vehicle, and another is a different position. The effectiveness of the proposed method is verified by numerical simulations considering sensor noises.

Key Words: Optic flow, Motion Estimation, Altitude Estimation, WFI of optic flow

Nomenclature

$\boldsymbol{F}$	:	sensitivity function
F	:	reference frame
$\boldsymbol{Q}$	:	position vector of a photoreceptor
$\dot{\boldsymbol{Q}}$	:	motion parallax vector
p	:	angular rate around x_b-axis
q	:	angular rate around y_b-axis
r	:	angular rate around z_b-axis
u	:	translational velocity along x_b-axis
$\boldsymbol{v}$	:	translational velocity vector w.r.t. F_b
v	:	translational velocity along y_b-axis
w	:	translational velocity along z_b-axis
$\boldsymbol{x}$	:	state variables
z	:	altitude
β	:	elevation angle
γ	:	azimuth angle
μ	:	nearness function
λ	:	numerator of nearness function
$\boldsymbol{\omega}$	:	rotational velocity vector w.r.t. F_b

Superscript

β	:	elevational direction
γ	:	azimuth direction

Subscripts

b	:	body fixed
t	:	terrain fixed

1. Introduction

For deep space exploration missions, autonomy is one of the key technologies because the time delay of commands from Earth is extremely long. Thus, in the vicinity of target celestial bodies, autonomous motion control of space probes should be established by using onboard sensors, because exogenous position sensors (e.g. Global Positioning System: GPS) cannot be used. Furthermore, such autonomous control systems are desirable to be light weight, small size, and low computation.

Wide-Field-Integration (WFI) of optic flow is one of the promising techniques, because it has the desirable features stated above. WFI of optic flow is a motion estimation method inspired by a biological research on the visual processing systems of flying insects' compound eyes.[1)-6)] Optic flow is the vector field of relative motion to environments, and the integration over a wide field of optic flow (i.e. WFI of optic flow) makes the motion estimation robust even in unknown environments. In the standard procedure for WFI of optic flow, the translational and rotational velocities of a vehicle are estimated by using other sensor outputs for the altitude and attitude information. Usually, the altitude is measured with a laser sensor, while the attitude information is obtained by Inertial Navigation System, e.g. accelerometer, gyroscope, magnetic sensor, etc.

This paper discusses a method to estimate not only the translational and rotational velocities but also the vehicle's altitude information.[7), 8)] The altitude estimation by WFI of optic flow are investigated as, 1) a backup system of a laser sensor, 2) an alternative method when a laser sensor is useless due to engine plume in a final touch down phase, and 3) expanded theory from academic viewpoints. First, the fundamental relation between vehicle's motion and optic flow obtained by a camera is generalized for arbitrary camera positions. Then, by utilizing two sets of optic flow obtained by two image sensors, the altitude estimation method is introduced. Finally, the proposed method is verified by numerical simulations considering sensor noises.

2. Estimation Procedure in Standard WFI of Optic Flow

This section first reintroduces the relation between a vehicle's motion and optic flow obtained. Then, a standard WFI of optic flow process is explained under the assumption that a camera is placed at the mass center of the vehicle.

2.1. Optic flow

Consider a vehicle moving a vicinity of a celestial surface, and define two reference frames: an inertial frame F_t fixed to the surface, and the vehicle fixed frame F_b whose origin is placed at the mass center of a vehicle (Fig. 1). The optic flow is the vector field of relative velocities between the vehicle and the environment.

Assume an image sensor is placed at the mass center of the vehicle, and its image surface is a sphere of unit radius denoted with S^2. Moreover, there are photoreceptors on the spherical image surface, and the positions of the photoreceptors are defined with the azimuth and elevation angles; these angles are both measured positive from the x_b- and z_b-axes of the frame F_b, respectively. Then, the position of a photoreceptor is described from two sequential rotations for the azimuth and elevation angles, γ and β, as follows:

$$\boldsymbol{Q} = \begin{bmatrix} \sin\beta\cos\gamma & \sin\beta\sin\gamma & \cos\beta \end{bmatrix}^T . \tag{1}$$

Consider that the fiducial point on the surface is stationary to F_t, and that the reference frame F_b fixed to the vehicle, which is moving with $\boldsymbol{v} = [u\ v\ w]^T$ and $\boldsymbol{\omega} = [\ p\ q\ r\ ]^T$. Then, the motion parallax vector $\dot{\boldsymbol{Q}}$ is defined as the time derivative of $\boldsymbol{Q}$ on the spherical imaging surface. Then optic flow can be expressed as [8)]

$$\dot{\boldsymbol{Q}} = -\boldsymbol{\omega}\times\boldsymbol{Q} - \mu\left\{\boldsymbol{v} - \left(\boldsymbol{v}^T\boldsymbol{Q}\right)\boldsymbol{Q}\right\}, \tag{2}$$

where μ is defined as the inverse of the distance to a point on the celestial surface. Then, the two component of optic flow along the azimuth and elevation directions can be expressed from Eq. (2) as follows.

$$\dot{Q}^{\gamma} = pc\beta c\gamma + qc\beta s\gamma - rs\beta + \mu\left(us\gamma - vc\gamma\right), \tag{3}$$

$$\dot{Q}^{\beta} = ps\gamma - qc\gamma - \mu\left(uc\beta c\gamma + vc\beta s\gamma - ws\beta\right), \tag{4}$$

where $c(*)$ and $s(*)$ indicate cos(*) and sin(*), respectively.

2.2. Motion estimation by WFI of optic flow

The research on optic flow has started over 50 years ago. [8)-10)] However, precise motion estimation by using optic flow is difficult, because optic flow is very sensitive to the uncertainty of surface profiles and sensor noises.

Thus, WFI of optic flow has been introduced to utilize a wide range of optic flow for better estimation. [11)-18)] The obtained optic flow is integrated with space functions $\boldsymbol{F}$, which are called "sensitivity functions". By using the sensitivity functions, sensor outputs y is obtained as follows:

$$y = \int_{S^2} \dot{\boldsymbol{Q}}^T \boldsymbol{F}\, d\Omega, \tag{5}$$

where $d\Omega = \sin\beta \cdot d\beta \cdot d\gamma$ is a solid angle on the spherical image surface. Furthermore, the space integration in Eq. (5) can be replaced with Riemann sum at the photoreceptor positions without degrading estimation accuracy, [15)] as follow.

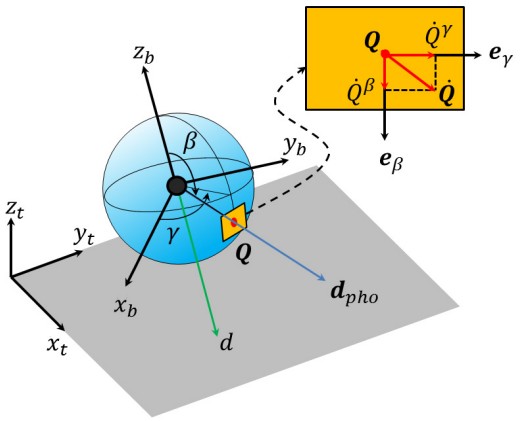

Fig.1. Spherical image model for WFI of optic flow.

$$y = \sum_{k=1}^{N} \dot{\boldsymbol{Q}}\left(\gamma_k,\beta_k\right)^T \boldsymbol{F}\left(\gamma_k,\beta_k\right)\Delta\Omega, \tag{6}$$

where $\left(\gamma_k,\beta_k\right)$ and N indicates the position and the number of the photoreceptors on the spherical image surface.

For three-dimensional motion estimation, spherical harmonics are frequently used as the sensitivity functions. Furthermore, to distinguish the azimuth and elevational directional components of optic flow, this study uses the following form of sensitivity functions. [19)]

$$\boldsymbol{F}_j = \begin{bmatrix} F_j^{\gamma} & 0 \\ 0 & F_j^{\beta} \end{bmatrix}, \tag{7}$$

where subscript j indicates the j-th spherical harmonics. Thus, by using up to M-th spherical harmonics, the following output vector is obtained for optic flow components measured by photoreceptors.

$$\boldsymbol{y} = \begin{bmatrix} \sum_{k=1}^{N} \dot{Q}^{\gamma}\left(\gamma_k,\beta_k\right) F_1^{\gamma}\left(\gamma_k,\beta_k\right)\Delta\Omega \\ \vdots \\ \sum_{k=1}^{N} \dot{Q}^{\gamma}\left(\gamma_k,\beta_k\right) F_M^{\gamma}\left(\gamma_k,\beta_k\right)\Delta\Omega \\ \sum_{k=1}^{N} \dot{Q}^{\beta}\left(\gamma_k,\beta_k\right) F_1^{\beta}\left(\gamma_k,\beta_k\right)\Delta\Omega \\ \vdots \\ \sum_{k=1}^{N} \dot{Q}^{\beta}\left(\gamma_k,\beta_k\right) F_M^{\beta}\left(\gamma_k,\beta_k\right)\Delta\Omega \end{bmatrix}. \tag{8}$$

On the other hand, WFI of optic flow virtually supposes a flat, infinite, and horizontal plane instead of uncertain surface profiles. Then, the nearness function μ in Eqs. (3) and (4) can be expressed as follows:

$$\mu = \frac{-s\beta c\gamma s\theta + s\beta s\gamma s\phi c\theta + c\beta c\phi c\theta}{z}, \tag{9}$$

where z is the "altitude" from the virtual plane, ϕ and θ are the roll and pitch angles of the vehicle expressed in the 3-2-1 Euler angle sequence. Thus, the output $\boldsymbol{y}$ in Eq. (8) can

be also evaluated from the flat surface assumption by using Eqs. (3), (4) and (9). The following 6-state variables appears linearly in the output equations,

$$\boldsymbol{x} = \begin{bmatrix} u & v & w & p & q & r \end{bmatrix}^T . \tag{10}$$

Thus, for the expression $\boldsymbol{y} = \boldsymbol{C}\boldsymbol{x}$, the standard procedure for WFI of optic flow can estimate the 6-motion variables by using the pseudo inverse matrix $\boldsymbol{C}^\dagger$ as follows:

$$\boldsymbol{x} = \boldsymbol{C}^\dagger \boldsymbol{y} . \tag{11}$$

3. Effect of Sensor Position on Optic Flow

In previous section, image sensors are assumed to be placed at the mass center of vehicles, and the optic flow measured by such cameras is expressed as Eq. (2). Here, the effect of the camera's position off from the mass center is discussed, and a simple countermeasure to cope with is introduced.

The first and second terms in the right hand side of Eq. (2) are linear for the angular and translational velocities, respectively. Thus, the equation can be rewritten in a simple form as

$$\dot{\boldsymbol{Q}} = \boldsymbol{A}\boldsymbol{\omega} + \frac{\lambda(\phi,\theta)}{z}\boldsymbol{B}\boldsymbol{v} , \tag{12}$$

where

$$\boldsymbol{A} = \begin{bmatrix} c\beta c\gamma & c\beta s\gamma & -s\beta \\ s\gamma & -c\gamma & 0 \end{bmatrix} , \quad \boldsymbol{B} = \begin{bmatrix} s\gamma & -c\gamma & 0 \\ -c\beta c\gamma & -c\beta s\gamma & s\beta \end{bmatrix},$$

and $\lambda(\phi,\theta)$ is the numerator in the right hand side of Eq. (9). The camera's position off from the vehicle's mass center effects in two parts of Eq. (12): altitude z and velocity vector $\boldsymbol{v}$. The altitude at the camera position is different from that at the mass center (see Fig. 2). Thus, in the same way as Eq. (1), define the vector $\boldsymbol{P}$ for the position of the camera w.r.t. F_b as

$$\boldsymbol{P} = P\begin{bmatrix} \sin\beta_\mathrm{c}\cos\gamma_\mathrm{c} & \sin\beta_\mathrm{c}\sin\gamma_\mathrm{c} & \cos\beta_\mathrm{c} \end{bmatrix}^T , \tag{13}$$

where P indicates the distance from the mass center, i.e. $P = |\boldsymbol{P}|$. Then, the altitude at the camera position can be described by considering the translational matrix from F_b to F_t, $\boldsymbol{R}^\mathrm{tb}$, as follows.

$$\begin{aligned} z_\mathrm{c} &= z + \left[\boldsymbol{R}^\mathrm{tb}\boldsymbol{P}\right]_\mathrm{z} \\ &= z + P\left(-s\theta s\beta_\mathrm{c}c\gamma_\mathrm{c} + c\theta s\phi s\beta_\mathrm{c}c\gamma_\mathrm{c} + c\phi c\theta c\beta_\mathrm{c}\right). \end{aligned} \tag{14}$$

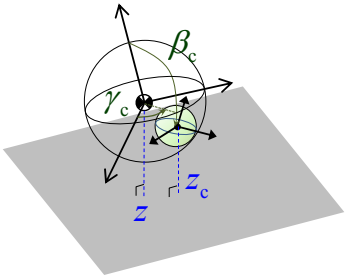

Fig.2. Spherical image plane placed off from the mass center of a vehicle.

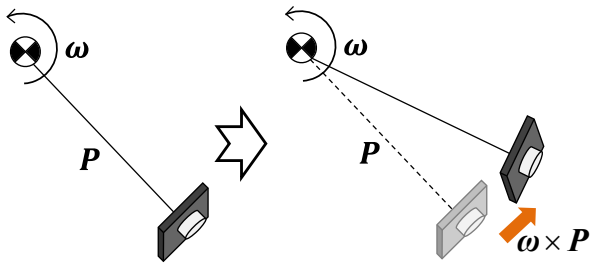

Fig.3. Camera's translational motion induced by a rotation around the mass center of a vehicle.

On the other hand, the camera's velocity vector $\boldsymbol{v}_\mathrm{c}$ can be expressed from Fig. 3 as follows:

$$\boldsymbol{v}_\mathrm{c} = \boldsymbol{v} + \boldsymbol{\omega}\times\boldsymbol{P} . \tag{15}$$

Thus, from Eqs. (12) and (15), the optic flow measured by a camera can be expressed by the following relation.

$$\dot{\boldsymbol{Q}} = \boldsymbol{A}\boldsymbol{\omega} + \frac{\lambda(\phi,\theta)}{z_\mathrm{c}}\left(\boldsymbol{B}\boldsymbol{v} + P\boldsymbol{B}\boldsymbol{C}\boldsymbol{\omega}\right), \tag{16}$$

where z_c is shown in Eq. (14) and $\boldsymbol{C}$ is a 3×3 matrix defined with the camera position.

From Eq. (16), the two components of optic flow can be expressed in the same way as Eqs. (3) and (4). Therefore, the motion estimation procedure explained in Subsection 2.2 can be expanded with small modifications for cameras placed off from the mass center of a vehicle.

4. Altitude Estimation Added to Motion Estimation

For the estimation of the vehicle's altitude from the ground, this section proposes an estimation procedure by using two set of optic flow measured by two cameras.

When one camera is assumed to be placed at the mass center of a vehicle, i.e. $P = 0$, the optic flow is expressed with Eq. (12). Then, define the following state variables instead of Eq. (10).

$$\boldsymbol{x}_1 = \begin{bmatrix} U & V & W & p & q & r \end{bmatrix}^T =: \begin{bmatrix} \boldsymbol{V}_1^T & \boldsymbol{\omega}_1^T \end{bmatrix}^T , \tag{17}$$

where $U = u/z$, $V = v/z$, and $W = w/z$. Then, since the vector $\boldsymbol{x}_1$ has six components, all of the elements can be estimated through a standard procedure for WFI of optic flow. Furthermore, assume that the vehicle has another camera placed off from the mass center. Thus, the optic flow measured by the second camera is described by Eq. (16).

Multiplying z_c in both sides of Eq. (16) leads the following relation:

$$\dot{\boldsymbol{Q}}z_\mathrm{c} = \boldsymbol{A}\boldsymbol{\omega}z_\mathrm{c} + \lambda\left(\boldsymbol{B}\boldsymbol{v} + P\boldsymbol{B}\boldsymbol{C}\boldsymbol{\omega}\right) . \tag{18}$$

Here, note that since the two cameras are boarded on a vehicle, the state variables estimated from the second camera should be same as those from the first one. Thus, the $\boldsymbol{V}_1$ and $\boldsymbol{\omega}_1$ estimated from the first sensor can be substituted into Eq. (18) considering $\boldsymbol{v} = z\boldsymbol{V}_1$. Then, the relation is

$$\dot{\boldsymbol{Q}}z_c = \boldsymbol{A}\boldsymbol{\omega}_1 z_c + \lambda\left(z\boldsymbol{B}\boldsymbol{V}_1 + P\boldsymbol{B}\boldsymbol{C}\boldsymbol{\omega}_1\right). \qquad (19)$$

Since z_c is shown in Eq. (14), the above relation includes only one unknown parameter z (Note, the second term in Eq. (14) can be evaluated as a constant value when the attitude angles ϕ and θ are measured by other sensors). Therefore, the altitude can be estimated from Eq. (19). Once z is obtained, then the translational velocities are calculated from $\boldsymbol{v} = z\boldsymbol{V}_1$. Thus, combining the estimation of $\boldsymbol{\omega}_1(=\boldsymbol{\omega})$, the altitude information and the six state variables can be estimated from two sets of optic flow measured by two cameras.

Note since the optic flow has two components, the altitude information from Eq. (19) can be evaluated in two ways: from the azimuth and from the elevation components. The point to be noted in this altitude estimation is explained in the next section.

5. Numerical Simulation

To verify the effectiveness of the proposed altitude estimation procedure added to the motion estimation, this section shows some typical numerical simulation results.

Note, in the simulations, the followings conditions are adopted for future experimental verification using a micro air vehicle and real optic flow sensors. First, the altitude and motion estimations of space vehicle are usually required at tens or hundreds meters height above planet surfaces. However, the vehicle altitude in the simulations is set as 1 [m] for the experiments. Next, the optic flow sensor shown in Fig. 4 will be used in the experiments. The sensor is OpticalFlow-Z made by ZMP Inc., and its processing algorithm has been improved to generate 79×59 optic flow vectors for the field of view 45.1 [deg] × 34.6 [deg] with a frame rate of 10 [fps]. Thus, the optic flow in the simulations is assumed to be obtained in the same conditions as the experimental sensor. Furthermore, the previous study [18] has implied that two optic sensors with 90 [deg]-interval in the azimuth direction show reasonable estimation accuracy for any directional translational motion of a vehicle. Thus, the camera positions in the simulation are supposed as shown in Table 1.

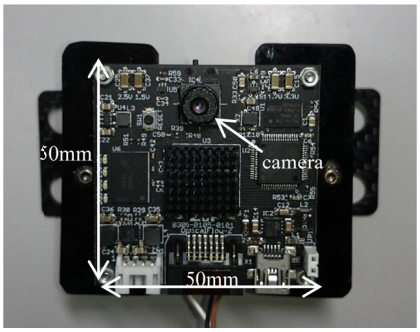

Fig.4. Optic flow sensor used in future experiments.

Table 1. Camera positions used in the simulation.

	Camera 1	Camera 2
Azimuth angle γ_c [deg]	0	90
Elevation angle β_c [deg]	135	135
Distance from c.m. R [m]	0	0.5

Table 2. Vehicle's motion parameters used in the simulations.

parameters	values
Altitude z [m]	1
Attitude angles (ϕ,θ,ψ) [deg]	(0, 0, 0)
Case 1: Translational velocities (u, v, w) [m/s]	(0.2, 0.2, 0)
Case 2: Translational velocities (u, v, w) [m/s]	(0.2, 0, 0)
Angular velocities (p, q, r) [rad/s]	(0, 0, 0)

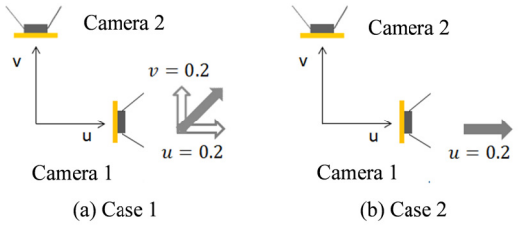

Fig.5. Vehicle's Translational velocities in two cases.

This paper shows the estimation results for the vehicle's two cases of motions shown in Table 2, which are same except the translational velocities. Figure 5 shows the geometric relations between the cameras and translational directions. Note that in each case, uniform random noises are added to both the azimuth and the elevation components of optic flow vectors. The maximum magnitude of random noises is specified with 30% of the magnitude of the exact optic flow, which should be measured in an ideal condition.

Figure 6 (a) and (b) show the estimated result of the vehicle's altitude in Case 1 from the azimuth and the elevation components of optic flow, respectively. Thus, for better estimation, usually the two estimated altitude should be averaged at each instant. Figure 7 indicates the estimated motion variables for the averaged altitude information. From Figs. 6 and 7, it is seen that both the altitude information and motion variables (translational and rotational velocities) can be estimated with reasonable accuracies by using two cameras.

On the other hand, Fig. 8 shows the estimated altitude information in Case 2. In this case, the estimation accuracy from the elevation component of optic flow is apparently worse. This reason can be explained from Fig. 9. As can be seen, the optic flow vectors measured by the camera 2 have small values in the elevational direction. Therefore, the estimation accuracy becomes lower. This implies one realistic procedure for the altitude estimation as follows. First, evaluate the magnitudes of two components of the obtained optic flow vectors, by sampling or by averaging. When both components are not sufficiently small, the altitude information is finalized by averaging the two estimations from the azimuth and elevation components. If one component is small enough, only another component should be used for the altitude estimation.

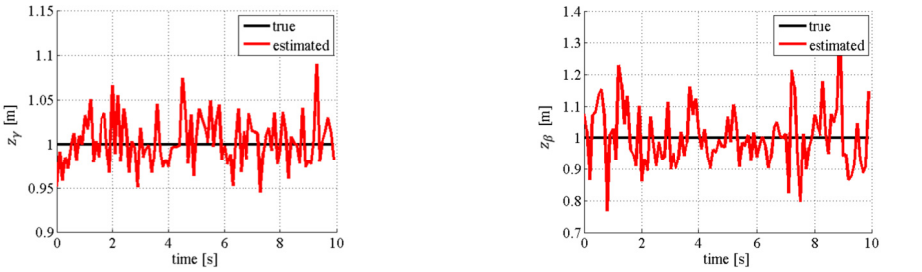

(a) Altitude estimation from γ component (b) Altitude estimation from β component

Fig.6. Vehicle's altitudes estimation from the azimuth and elevation components of optic flow (Case 1).

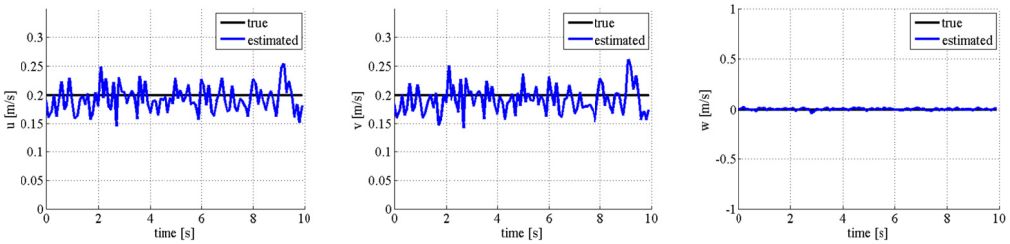

(a) Estimated translation velocities (left: u, center: v, right: w)

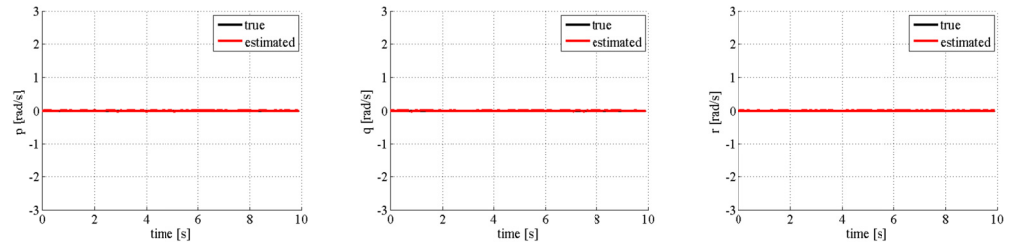

(b) Estimated angular velocities (left: p, center: q, right: r)

Fig.7. Vehicle's motion variables estimated from WFI of optic flow (Case 1).

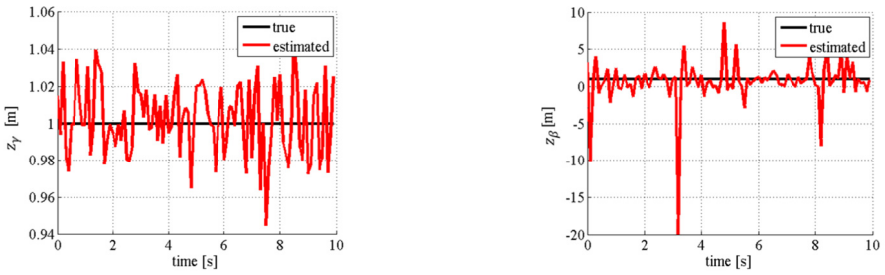

(a) Altitude estimation from γ component (b) Altitude estimation from β component

Fig.8. Vehicle's altitudes estimation from the azimuth and elevation components of optic flow (Case 2).

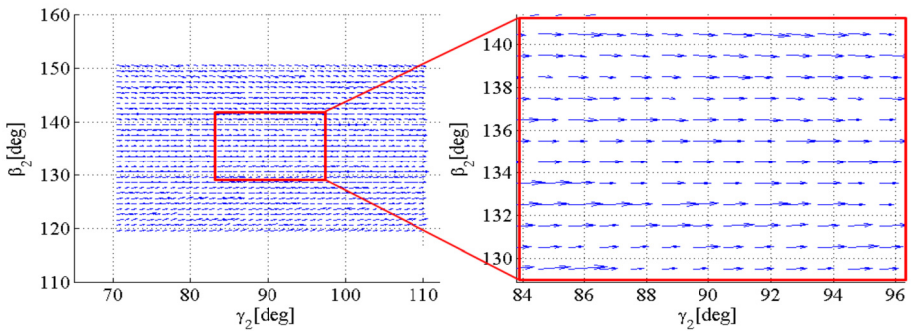

Fig.9. Optic flow and its enlargement captured by the camera 2 in Case 2.

6. Conclusion

This paper proposed a procedure to estimate both the vehicle's altitude and its translational and rotational velocities by using two cameras. For this purpose, the relation between optic flow and the vehicle's motion has been expanded so that they can deal with cameras placed off from the mass center of a vehicle. Then the estimation procedure has been introduced. The effectiveness of the proposed method has been verified by numerical simulations considering sensor noises.

Acknowledgments

This research is supported by Japan Society for the Pro-motion of Science (JSPS) KAKENHI Grant-in-Aid for Challenging Exploratory Research No. 15K14254, and by Sekisui Chemical Grant Program for Research on Manufacturing Based on Innovations Inspired by Nature.

References

1) Humbert, J. S.,: Bio-Inspired Visuomotor Convergence in Navigation and Flight Control Systems, Ph.D. Dissertation, Mechanical Engineering, Department, California Inst. of Technology, Pasadena, CA, 2006.
2) Humbert J. S., Murray R. M. and Dickinson M. H.: A Control-Oriented Analysis of Bio-inspired Visuomotor Convergence, Proceedings of the IEEE Conference on Decision and Control, pp. 245-250, 2005.
3) Humbert J. S. and Frye M. A.: Extracting Behaviorally Relevant Retinal Image Motion Cues via Wide-Field Integration, Proceedings of the American Control Conference, pp.2724-2729, 2007.
4) Epstein M., Waydo S., et al.: Biologically Inspired Feedback Design for Drosophila Flight, Proceedings of the American Control Conference, pp.3395-3401, 2007.
5) Conroy, J., Gremillion, G., Ranganathan, B. and Humbert, J. S.: Implementation of Wide-Field Integration of Optic Flow for Autonomous Quadrotor Navigation, Autonomous Robots. 27, No. 3, pp. 189-198, 2009.
6) Kobayashi N., Oishi M., Kinjo Y., Kubo D., and Hokamoto S: Motion estimation of autonomous spacecraft near asteroid using wide-field-integration of optic flow, Proceedings of the 25th International Symposium on Space Flight Dynamics, USB, pp.1-10, 2015.
7) Nakata R., Kobayashi N., Bando M., and Hokamoto S.: Altitude and motion estimation for small UAVs by using optic flow, Proceedings of the 8th KAIST-Kyushu University Symposium on Aerospace Engineering, 2016.
8) Gibson, J., The Perception of the Visual World, Houghton Mifflin, Oxford, England, U.K., pp. 117–144, 1950.
9) Koenderink J. J. and van Doorn A. J.: Facts on Optic Flow, Journal of Biological Cybernetics, 56, pp.247-254, 1987.
10) Egelhaaf, M., Kern, R., Krapp, H. G., Kretzberg, J., Kurtz, R. and Warzecha, A.: Neural encoding of behaviourally relevant visual-motion information in the fly, Trends in Neurosciences, 25, pp. 96-102, 2002.
11) Hyslop, A. M., and Humbert, J. S.,: Autonomous Navigation in Three-Dimensional Urban Environments Using Wide-Field Integration of Optic Flow, Journal of Guidance, Control, and Dynamics, Vol. 33, No. 1, pp. 147–159, 2010.
12) Hyslop A. M., Krapp H. G. and Humbert J. S.: Control theoretic interpretation of directional motion preferences in optic flow processing interneurons, Journal of Biological Cybernetics, Vol. 103, pp.353-364, 2010.
13) Shoemaker M. A. and Hokamoto S.: Application of Wide-Field Integration of Optic Flow to Proximity Operations and Landing for Space Exploration Missions, Advances in the Astronautical Sciences, Vol. 142, pp.23-36, 2011.
14) Izzo, D., Weiss, N. and Seidl, T.: Constant-Optic-Flow Lunar Landing: Optimality and Guidance, Journal of Guidance, Control, and Dynamics, 34, No. 5, pp. 1383-1395, 2011.
15) Shoemaker, M. A. and Hokamoto, S.: Comparison of Integrated and Non-integrated Wide-Field Optic Flow for Vehicle Navigation, Journal of Guidance, Control, and Dynamics, Vol. 36, No.3, pp.710-720.2013.
16) Sakamoto H., and Hokamoto S.: Attitude Angle Estimation of Space Probe through Wide-Field Integration of Optic Flow, Transactions of the Japan Society for Aeronautical and Space Sciences, Aerospace Technology Japan, Vol. 12, No. ists29 pp.Pd_41-Pd_46, 2014
17) Kobayashi N., Nakata R., Bando M., and Hokamoto S.: A Novel Attitude Estimation Method Based on Wide-Field-Integration of Optic Flow for Autonomous Navigation, Proceedings of the 2016 Asia-Pacific International Symposium on Aerospace Technology (APISAT), 2016.
18) Kobayashi N., Oishi M., Kinjo Y., and Hokamoto S.: Experimental verification of wide-field-integration of optic flow for state estimation, Transactions of the Japan Society for Aeronautical and Space Sciences, Aerospace Technology Japan, Vol.14, No. ists30, Pd_63-Pd_68, 2016.
19) Kobayashi N., Bando M., Hokamoto S.: Improvement of Wide-Field-Integration of Optic Flow Considering Practical Sensor Restrictions, Journal of Mechanics Engineering and Automation, (accepted)